

Lawrence Berkeley National Laboratory

Molecular Biophys & Integ Bi

Title

A platinum catalyst deposited on a zirconia support for the design of lithium-oxygen batteries with enhanced cycling ability

Permalink

<https://escholarship.org/uc/item/4vj4z4g6>

Journal

Chemical Communications, 53(86)

ISSN

1359-7345

Authors

Bae, Seongjun
Geun Yoo, Young
Park, Jongseok
[et al.](#)

Publication Date

2017-08-22

DOI

10.1039/c7cc05459a

Peer reviewed



Cite this: *Chem. Commun.*, 2017, 53, 11767

Received 14th July 2017,
Accepted 5th October 2017

DOI: 10.1039/c7cc05459a

rsc.li/chemcomm

A platinum catalyst deposited on a zirconia support for the design of lithium–oxygen batteries with enhanced cycling ability†

Seongjun Bae,^{ab} Young Geun Yoo,^{ab} Jongseok Park,^{ab} Soomin Park,^{ab} Inho Nam,^{ab} Jeong Woo Han^{id} ^c and Jonghoep Yi^{id} ^{*ab}

A platinum catalyst supported on zirconia is proposed as a cathode in lithium–oxygen batteries. Experimental and theoretical studies show that zirconia suppresses the side-reactions of the intermediate (O_2^-) and the final product (Li_2O_2) by the stabilization of their reactivity. Thus, it is able to enhance the reversibility during charge/discharge in lithium–oxygen batteries.

Current advances in electric devices have increased the demand for next-generation electric energy storage systems. However, the conventional lithium-ion batteries (LIBs) have reached their theoretical limits. Their power and energy are not enough for application in next-generation electric devices, such as electric vehicles (EVs).^{1–3} Therefore, alternative battery systems have been proposed and investigated as replacements for LIBs.^{4–6}

A lithium–oxygen ($\text{Li}-\text{O}_2$) battery is a highly promising candidate to replace conventional LIBs, because the theoretical energy density of $\text{Li}-\text{O}_2$ batteries is much higher than that of LIBs (3500 W h kg^{-1}).⁷ However, the high overpotential and low cycle life have impeded the practical use of $\text{Li}-\text{O}_2$ batteries. One of the causes of the impediment is that the Li_2O_2 decomposition reaction during the charging process is highly resistive due to the low electric conductivity of Li_2O_2 . Also, side reactions can occur on the cathode where the lithium ion reacts with external oxygen resulting in lithium peroxide (Li_2O_2). Because superoxide and peroxide species (SPS, O_2^- , LiO_2 and Li_2O_2) are not stable, they can easily react with the electrolyte and carbon electrode, which results in the passivation of the cathode and a higher decomposing potential compared to that of Li_2O_2 .^{8–10}

Various catalysts have been proposed for $\text{Li}-\text{O}_2$ batteries to solve the issues regarding high overpotential and low cycle

lives.^{11–14} Among them, noble metal catalysts (NMCs) have shown remarkable performance due to their high catalytic activity which could reduce the overpotential.^{15–17} However, NMCs not only catalyze the Li_2O_2 decomposition, but also promote side-reactions, because the catalytic behavior of NMCs is not selective.^{18,19} Byproducts from the side-reactions increase the interfacial resistance which has a negative influence on the cycling ability and causes a gradual increase in the overpotential.^{20–22} Therefore, the stabilization of SPS is the key strategy for stable and reversible reactions of NMCs in $\text{Li}-\text{O}_2$ batteries.

Designing a cathode material of $\text{Li}-\text{O}_2$ batteries could be a solution to relieve the side reactions. Several types of metal oxides are known to stabilize the SPS *via* oxygen defects on the surface.^{23,24} Because SPS are nucleophilic, they easily bind with oxygen defect sites, which could suppress their reactivity. Adaptation of the surface properties of these metal oxides is necessary to suppress the byproduct formation. Therefore, the concept of hybridization between highly active NMCs and the SPS-stabilizing metal oxides should be pursued.

In this research, a platinum catalyst deposited onto zirconia is proposed for our proof-of-concept model to establish the synergetic effect of NMCs and an oxygen-defective support. We chose zirconia as a support because it offers oxygen defects on the surface without providing additional oxygen reduction/evolution reaction sites during charge/discharge. Therefore, reactions occur mainly on the platinum surface. We observed the effect of the support with oxygen defects using experimental and theoretical approaches relative to the performance of $\text{Li}-\text{O}_2$ batteries. As a result, Pt/ZrO_2 exhibited longer cyclability compared to a sole platinum catalyst. The electrochemical and physicochemical properties of both catalysts and the discharged products were characterized *via* experimental and theoretical methods to investigate the origins of the longer cyclability. The oxygen defect site of the zirconia support improved the reversibility by interacting with discharge products.

To compare the morphology of Pt/ZrO_2 and Pt particles, transmission electron microscopy (TEM) images were obtained. The TEM images revealed that platinum particles of similar size

^a School of Chemical and Biological Engineering, Seoul National University, Seoul 151-742, Republic of Korea. E-mail: jyi@snu.ac.kr

^b World Class University (WCU) Program of Chemical Convergence for Energy & Environment (C2E2), Institute of Chemical Processes, Seoul National University, Seoul 151-742, Republic of Korea

^c Department of Chemical Engineering, University of Seoul, Seoul 130-743, Republic of Korea

† Electronic supplementary information (ESI) available. See DOI: 10.1039/c7cc05459a

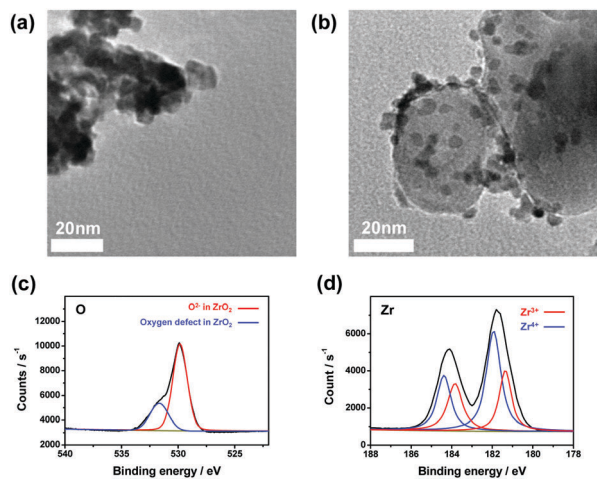


Fig. 1 TEM images of (a) Pt particles and (b) Pt/ZrO₂, and XPS analysis of (c) O1s and (d) Zr3d orbital of Pt/ZrO₂.

(less than 10 nm) and shape were dispersed uniformly onto larger (approximately 50 nm) zirconia particles of Pt/ZrO₂ (Fig. 1a). Pure Pt particles are similar in size and shape compared to those that were deposited onto the zirconia (Fig. 1b). This suggests that the morphological differences in the active sites between Pt/ZrO₂ and Pt particles are negligible. X-ray diffraction (XRD) patterns showed the crystallinity of the Pt/ZrO₂ and Pt particles (Fig. S1, ESI†). Both samples had the same face-centered cubic crystalline platinum peaks (JCPDS, Card no. 04-0802), which can be attributed to the (111) and (200) planes. The crystal structure of zirconia was characterized as purely monoclinic (JCPDS, Card no. 37-1484). BET surface area analysis also verified that the surface area effect could be ignored. The BET specific surface areas of the Pt/ZrO₂ and Pt particles were 22.6 cm² g⁻¹ and 15.1 cm² g⁻¹, respectively. Pore structures were not developed on the surfaces of either Pt/ZrO₂ or Pt particles, which indicates that the prepared materials are conventional metal oxide and metal particles (Fig. S2, ESI†).

The oxidation states of the surface atoms of Pt/ZrO₂ were characterized *via* XPS. O1s, Zr3d and Pt4f orbitals of Pt/ZrO₂ are described in Fig. 1c, d and Fig. S3 (ESI†). The peak of the O1s orbital was deconvoluted into two parts, 529.8 eV and 531.7 eV. The binding energy at 529.8 eV is associated with the oxygen ion in the lattice of zirconia and that at 531.7 eV is interpreted as the oxygen defect or adsorbed species on the surface of zirconia.^{25–27} Physisorbed species can be easily removed by the vacuum conditions of XPS analysis. Therefore, any observed oxygen is from chemisorbed species such as a hydroxyl group or water, which bind mostly with the oxygen defects on zirconia. Therefore, the peak at 531.7 eV is directly related to the oxygen defect. The evolved peaks at 181.9/184.4 eV and 181.4/183.8 eV were assigned to Zr⁴⁺ and Zr³⁺, respectively. The peaks at 70.3/73.7 eV (red line), 71.5/74.9 eV (blue line) and 72.6/75.9 eV (green line) are assigned to Pt⁰, Pt²⁺ and Pt⁴⁺, respectively.

The electrochemical performance of Pt/ZrO₂ used as a catalytic cathode for Li–O₂ batteries was evaluated *via* a galvanostatic charge/discharge test at a current density of 0.2 mA cm⁻²,

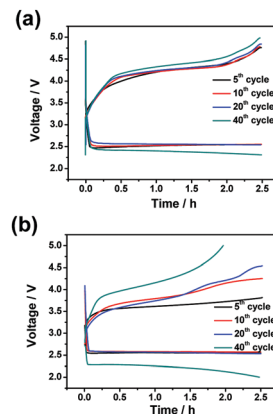


Fig. 2 Charge/discharge test at 0.2 mA cm⁻² of (a) 10 wt% Pt/ZrO₂ and (b) Pt particles.

in a voltage window of 2.0–5.0 V and with a limited time of 2.5 h (cut-off capacity of 1000 mA h g⁻¹). An electrochemical test of Pt particles was also conducted using the same conditions. As shown in Fig. 2a and b, at the first cycle, the discharging/charging potentials of Pt/ZrO₂ and Pt were observed at 2.7/4.2 V and 2.7/3.5 V, respectively. Even the charging overpotential of Pt was relatively lower than that of Pt/ZrO₂ at the initial few cycles; however, it dramatically increased from the 5th cycle and a fast degradation of performance was observed near the 40th cycle. In contrast, Pt/ZrO₂ maintained a flat charge profile and a capacity even after the 40th cycle.

Since the charging potential is closely related to the oxidation of a discharge product, the low initial overpotential of the Pt particle indicates that it definitely catalyzes the oxidation reaction. However, as the cycle proceeded, both the charging potential and the variation in the potential profile drastically worsened. As stated at the beginning, this phenomenon is due to the formation of byproducts from undesired reactions by the platinum catalyst.^{18,19} The Pt/ZrO₂, on the other hand, maintained its performance for longer cycles. The consistent charging profiles of Pt/ZrO₂ suggest that less byproducts were formed with Pt/ZrO₂. Based on these results, the better cyclability of the platinum with a zirconia support can be explained by the highly reversible Li–O₂ redox chemistry without side-reactions.

To investigate the effect of the zirconia as a support material for a platinum catalyst, the reactivities of the intermediates and final discharge products of Li–O₂ batteries were investigated. Because SPS undergo nucleophilic attack with electrolytes and a carbon-based electrode during charge/discharge reactions, measuring the stability of SPS could be the criterion for the reversibility of the charge/discharge reactions. Fig. 3a shows the results of the galvanostatic reduction/oxidation test of Pt/ZrO₂ and Pt particles under 0.5 M tetrabutylammonium (TBA) salt. The Pt/ZrO₂ group exhibits higher overpotential than the Pt particle due to the low conductivity of the zirconia support. Because LiO₂ and Li₂O₂ cannot be formed under these conditions, only O₂⁻ is observed. Even with TBA, O₂⁻ still maintains its reactivity toward the electrolyte. Therefore, the amount of re-oxidized O₂⁻ is always smaller than the reduced O₂⁻, and the

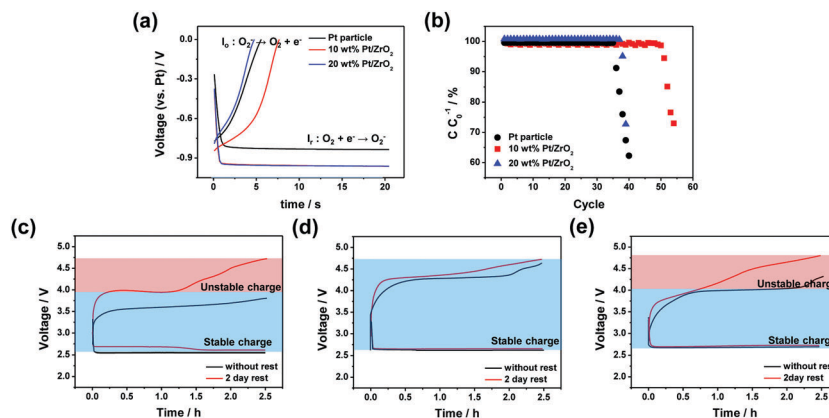


Fig. 3 (a) Galvanostatic charge/discharge test of 10, 20 wt% Pt/ZrO₂ and Pt particles under tetrabutylammonium (TBA) salt at 5 μ A, (b) cyclability of samples with 10, 20 wt% Pt/ZrO₂ and Pt particles, and charge/discharge test without rest and with 2 days of rest between the charge and discharge processes of (c) Pt particles, (d) 10 wt% Pt/ZrO₂ and (e) 20 wt% Pt/ZrO₂.

oxygen collection efficiency indicates the side-reaction rate of O₂⁻. The ratio of re-oxidation and reduction currents (I_o/I_r) increased from 28.4% (Pt particle) to 38.5% (10 wt% Pt/ZrO₂), which implies that O₂⁻ consumption is suppressed by the zirconia support. Oxygen defects on the exposed surface of zirconia function as binding sites for O₂⁻, which mitigates the reactivity of O₂⁻. Therefore, the reaction between O₂⁻ and an electrolyte is diminished in Pt/ZrO₂. However, as the Pt content in Pt/ZrO₂ is increased from 10 to 20 wt%, the oxygen collection efficiency was decreased to 24.7%. This is because the oxygen defects on the exposed zirconia surface and the binding sites for O₂⁻ were decreased as shown in the TEM image. As expected, the oxygen collection efficiency and cyclability of the samples have the same tendency (Fig. 3b). It is clear that the stabilization of O₂⁻ is a critical factor for the reversibility of a charge/discharge reaction, which defines the cyclability of Li-O₂ batteries.

Side-reactions also occur on the surface of the final discharge product, Li₂O₂. To investigate the reactivity of Li₂O₂ in the presence of the prepared catalysts, the Li-O₂ batteries with Pt/ZrO₂ and Pt particles were rested for 2 days after discharging (Fig. 3c–e). Without rest, the flat charging potential plateau of the Pt particle was observed at 3.5 V. After 2 days of rest, however, it was increased up to 4 V with a sloped profile. 20 wt% Pt/ZrO₂, which has a less exposed zirconia defect site than that of 10 wt% Pt/ZrO₂, showed the charging potential plateau at 4 V. In contrast, after 2 days of rest, the charging potential was increased and showed a sloped profile above 4 V. In contrast, the charging potentials of 10% Pt/ZrO₂ with and without a rest of 2 days were similar and flat-shaped near 4.2 V. According to the previous studies, a larger amount of CO₂ gas was observed during the sloped charge region that was originated from the decomposition of Li₂CO₃, which is a byproduct.^{28–30} Therefore, the appearance of a sloped charge potential curve indicates that a portion of Li₂O₂ has converted into Li₂CO₃ during the rest time. These results provide evidence that Li₂O₂ is unstable and converted into another chemical on the platinum surface, but is stable on a zirconia surface that suppresses side-reactions. As shown by the galvanostatic reduction/oxidation test results under TBA salt,

the zirconia support enables reversible reactions by stabilizing the intermediate and final-discharge products in Li-O₂ batteries.

Density functional theory (DFT) calculations were carried out to show the detailed interactions of Li₂O₂ adsorbed onto platinum (111) and zirconia (-111) planes, respectively, which are the most stable and abundant facets of each compound (Fig. 4).^{31,32} The adsorption energies of a Li₂O₂ monomer on platinum and zirconia were calculated to be -3.15 eV and -7.97 eV, respectively. The calculated values of binding energies of a dimer and a trimer also show that Li₂O₂ was adsorbed more strongly on the surface of zirconia. Since the adsorption energy of Li₂O₂ is related to its stability, the reactivity of Li₂O₂ is suppressed on the zirconia surface. The charging density difference between a Li₂O₂ trimer under vacuum and a Li₂O₂ trimer adsorbed onto platinum and zirconia surfaces shows the interaction of Li₂O₂ with these surfaces. The polarization of Li₂O₂ increases on the surface of platinum, which means a stronger nucleophilic attack could occur. By contrast, Li₂O₂ interacts

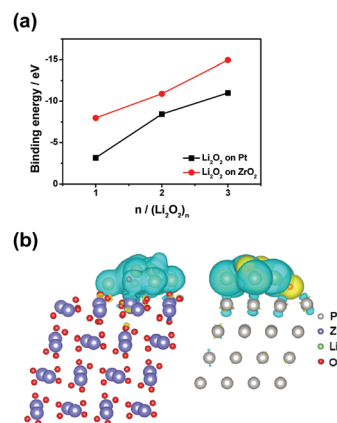


Fig. 4 Calculated binding energy of (Li₂O₂)_n ($n = 1, 2, 3$). Binding energy calculated by $E_{\text{Li}_2\text{O}_2} + E_{\text{surface}} - E_{\text{ad}}$, where $E_{\text{Li}_2\text{O}_2}$ is the energy of Li₂O₂ monomer, dimer and trimer, E_{surface} is the energy of clean surfaces of Pt and ZrO₂ and E_{ad} is the energy of Li₂O₂ adsorbed on Pt and ZrO₂. (b) Charge density difference of Li₂O₂ adsorbed on Pt and ZrO₂. The isosurfaces are 0.01 e⁻ Å⁻³ and plotted at positive (yellow) and negative (blue) values.

strongly with zirconia and is stabilized by losing the electron density. As the nucleophilicity of Li_2O_2 is reduced, its reactivity toward an electrolyte or electrode could be suppressed. The results on the platinum (200) and zirconia (111) planes, which are the second most stable and abundant planes, also showed analogous tendency (Fig. S5, ESI[†]). Therefore, these phenomena would be general on the surfaces of platinum and zirconia.

We also calculated the solvation energy of Li_2O_2 in a tetraethylene glycol dimethyl ether (TEGDME) electrolyte, which is calculated to be 1.73 eV. The adsorption energies of both platinum and zirconia surfaces to lithium superoxide are stronger than the solvation energy of TEGDME to lithium superoxide. Therefore, lithium superoxide is adsorbed on the surface rather than dissolved in the electrolyte, which agrees with previous studies. In the case of an electrolyte with a low donor number, Li_2O_2 grows on the surface of the electrode without the solvation of the electrolyte.^{33,34}

In summary, we investigated zirconia as a cathodic supporting material to establish the effect of oxygen-defective sites for a reversible charge/discharge reaction in Li–O₂ batteries. As a result, platinum deposited onto zirconia demonstrated an enhanced cyclability compared to that of a pure platinum catalyst. The improved reversibility can be explained by a stabilization of the nucleophilic species on zirconia. Although several design principles such as composition and morphology of active sites are important for the development of a catalyst for Li–O₂ batteries, the surface properties of the support are also critical to the electrochemical performance. This study may provide clues for the design of superior supporting materials for Li–O₂ batteries. Even by suppressing the side reactions by zirconia, the cyclability was only increased by 10 cycles compared to pure Pt in our study. We assumed that the low conductivity of the zirconia support has been one of the bottlenecks for the development of an electrocatalyst with even greater cyclability. We used simple sphere-type zirconia particles to establish the effect of a support with oxygen defects. Modification of the morphology such as the hybridization of the oxygen defective zirconia support and conductive carbon could enhance the performance of the catalyst.

This work was supported by the National Research Foundation of Korea (NRF) grant funded by the Korea government (MEST) (NRF-2016R1E1A1A01942936) and the Supercomputing Center/Korea Institute of Science and Technology Information with supercomputing resources including technical support (KSC-2016-C2-0058).

Conflicts of interest

There are no conflicts to declare.

Notes and references

- 1 Y. Wang, Z. Yang, Y. Quan, L. Gu and H. Zhou, *Adv. Mater.*, 2015, **27**, 3915–3920.
- 2 V. Etacheri, R. Marom, R. Elaari, G. Salitra and D. Aurbach, *Energy Environ. Sci.*, 2011, **4**, 3243–3262.
- 3 L. Peng, Y. Zhu, D. Chen, R. S. Ruoff and G. Yu, *Adv. Energy Mater.*, 2016, **6**, 1600025.
- 4 B. Dunn, H. Kamath and J. M. Tarascon, *Science*, 2011, **334**, 928–935.
- 5 D. Larcher and J. M. Tarascon, *Nat. Chem.*, 2015, **7**, 19–29.
- 6 J. W. Choi and D. Aurbach, *Nat. Rev. Mater.*, 2016, **1**, 16013.
- 7 J. Bao, W. Xu, P. Bhattacharya, M. Stewart, J. G. Zhang and W. Pan, *J. Phys. Chem. C*, 2015, **119**, 14851–14860.
- 8 B. D. McCloskey, A. Valery, A. C. Luntz, S. R. Gowda, G. M. Wallraff, J. M. Garcia, T. Mori and L. E. Krupp, *J. Phys. Chem. Lett.*, 2013, **4**, 2989–2993.
- 9 X. Yao, Q. Dong, Q. Cheng and D. Wang, *Angew. Chem., Int. Ed.*, 2016, **55**, 11344–11353.
- 10 R. A. Wong, A. Dutta, C. Yang, K. Yamanaka, T. Ohta, A. Nakao, K. Waki and H. R. Byon, *Chem. Mater.*, 2016, **28**, 8006–8015.
- 11 Z. L. Wang, D. Xu, J. J. Xu and X. B. Zhang, *Chem. Soc. Rev.*, 2014, **43**, 7746–7786.
- 12 N. Feng, P. He and H. Zhou, *Adv. Energy Mater.*, 2016, **6**, 1502303.
- 13 K. N. Jung, J. Kim, Y. Yamauchi, M. S. Park, J. W. Lee and J. H. Kim, *J. Mater. Chem. A*, 2016, **4**, 14050–14068.
- 14 B. Y. Xia, Y. Yan, N. Li, H. B. Wu, X. W. Lou and X. Wang, *Nat. Energy*, 2016, **1**, 15006.
- 15 F. Wu, Y. Xing, X. Zeng, Y. Yuan, X. Zhang, R. Shahbazian-Yassar, J. Wen, D. J. Miller, L. Li, R. Chen, J. Lu and K. Amine, *Adv. Funct. Mater.*, 2016, **26**, 7626–7633.
- 16 J. Cao, S. Liu, J. Xie, S. Zhang, G. Cao and X. Zhao, *ACS Catal.*, 2015, **5**, 241–245.
- 17 J. Yin, B. Fang, J. Luo, B. Wanjala, D. Mott, R. Loukrakpam, M. S. Ng, Z. Li, J. Hong, M. S. Whittingham and C. J. Zhong, *Nanotechnology*, 2012, **23**, 305404.
- 18 Y. S. Jeong, J. B. Park, J. G. Jung, J. Kim, X. Luo, J. Lu, L. Curtiss, K. Amine, Y. K. Sun, B. Scrosati and Y. J. Lee, *Nano Lett.*, 2015, **15**, 4261–4268.
- 19 S. Ma, Y. Wu, J. Wang, Y. Zhang, Y. Zhang, X. Yang, Y. Wei, P. Liu, J. Wang, K. Jiang, S. Fan, Y. Xu and Z. Peng, *Nano Lett.*, 2015, **15**, 8084–8090.
- 20 F. Li, T. Zhang and H. Zhou, *Energy Environ. Sci.*, 2013, **6**, 1125–1141.
- 21 D. Aurbach, B. D. McCloskey, L. F. Nazar and P. G. Bruce, *Nat. Energy*, 2016, **1**, 16128.
- 22 F. Li and J. Chen, *Adv. Energy Mater.*, 2017, 1602934 in press.
- 23 E. Carter, A. F. Carley and D. M. Murphy, *J. Phys. Chem. C*, 2007, **111**, 10630–10638.
- 24 K. Sobanska, A. Krasowska, T. Mazur, K. Podolska-Seraphin, P. Pietrzyk and Z. Sojka, *Top. Catal.*, 2015, **58**, 796–810.
- 25 A. V. Singh, M. Ferri, M. Tamplonizza, F. Borghi, G. Divitini, C. Ducati, C. Lenardi, C. Piazzoni, M. Merlini, A. Podesta and P. Milani, *Nanotechnology*, 2012, **23**, 475101.
- 26 Y. Lu, Z. Wang, S. Yuan, L. Shi, Y. Zhao and W. Deng, *RSC Adv.*, 2013, **3**, 11707–11714.
- 27 A. Sinhamahapatra, J. P. Jeon, J. Kang, B. Han and J. S. Yu, *Sci. Rep.*, 2016, **6**, 27218.
- 28 B. D. McCloskey, A. Speidel, R. Scheffler, D. C. Miller, V. Viswanathan, J. S. Hummelshoj, J. K. Norskov and A. C. Luntz, *J. Phys. Chem. Lett.*, 2012, **3**, 997–1001.
- 29 S. J. Kang, T. Mori, S. Narizuka, W. Wilche and H. C. Kim, *Nat. Commun.*, 2014, **5**, 3937.
- 30 D. W. Kim, S. M. Ahn, J. Kang, J. Suk, H. K. Kim and Y. Kang, *J. Mater. Chem. A*, 2016, **4**, 6332–6341.
- 31 N. E. Singh-Miller and N. Marzari, *Phys. Rev. B: Condens. Matter Mater. Phys.*, 2009, **80**, 235407.
- 32 A. Christensen and E. A. Carter, *Phys. Rev. B: Condens. Matter Mater. Phys.*, 1998, **58**, 8050–8064.
- 33 L. Johnson, C. Li, Z. Liu, Y. Chen, S. A. Freunberger, P. C. Ashok, B. B. Praveen, K. Dholakia, J. M. Tarascon and P. G. Bruce, *Nat. Chem.*, 2014, **6**, 1091–1099.
- 34 A. Khetan, A. Luntz and V. Viswanathan, *J. Phys. Chem. Lett.*, 2015, **6**, 1254–1259.